Chapter 4
Synthesised Structures *N,N'*-bis(γ-butyric)-pyromellitic diimide and its Charge Transfer Complexes

4.1 Introduction

Derivatives of pyromellitic diimides are of vast importance as they can lead to the formation of new arrays in host-guest chemistry (Park *et al*., 2003). Their electrophilic character allows for the attraction of nucleophilic aromatic rings. These non covalent type interactions are important as they allows new functional materials to be designed (Barooah *et al*., 2006). In this chapter, the structural and physical features of a new host molecule *N,N'*-bis(γ-butyric)-pyromellitic diimide and CT complexes will be discussed.

4.2 Experimental

4.2.1 Synthesis of *N,N'*-bis(γ-butyric)-pyromellitic diimide (but-L)

Pyromellitic dianhydride (1.09 g, 5mmol) and γ-aminobutyric acid (0.75 g, 10mmol) were added to a 200ml round bottom flask containing boiling stones and 30ml glacial acetic acid. The resulting mixture was allowed to reflux for approx. 10-12 hours at 130°C. The product was filtered and washed in cold methanol and acetone, to remove any starting material residue, and recrystallised in DMF. Crystals were obtained in clusters along the rim as the solvent evaporated, with a yield of 90%.

4.2.2 Charge Transfer complexes

CT complexes using *N,N'*-bis(γ-butyric)-pyromellitic diimide (but-L) were synthesised by dissolving 49mg of ligand into 3ml dimethylformamide. This solution was then added to the appropriate aromatic donor (naphthalene, anthracene, phenanthrene and perylene) contained in 5ml chloroform, resulting in a layered solution, forming a 1:1 molar complex. . The mixture was then allowed to evaporate in the fume hood. Unfortunately attempts to grow CT complexes containing anthracene and naphthalene were unsuccessful.

4.3 Crystal Morphology

4.3.1 but-L with Various Aromatic Guests

Crystal morphology and colour was observed using a Olympus SZ60 microscope at 50x magnification. The resulting images made it possible to examine the differences in colour and crystal morphology for all CT complexes formed with but-L.

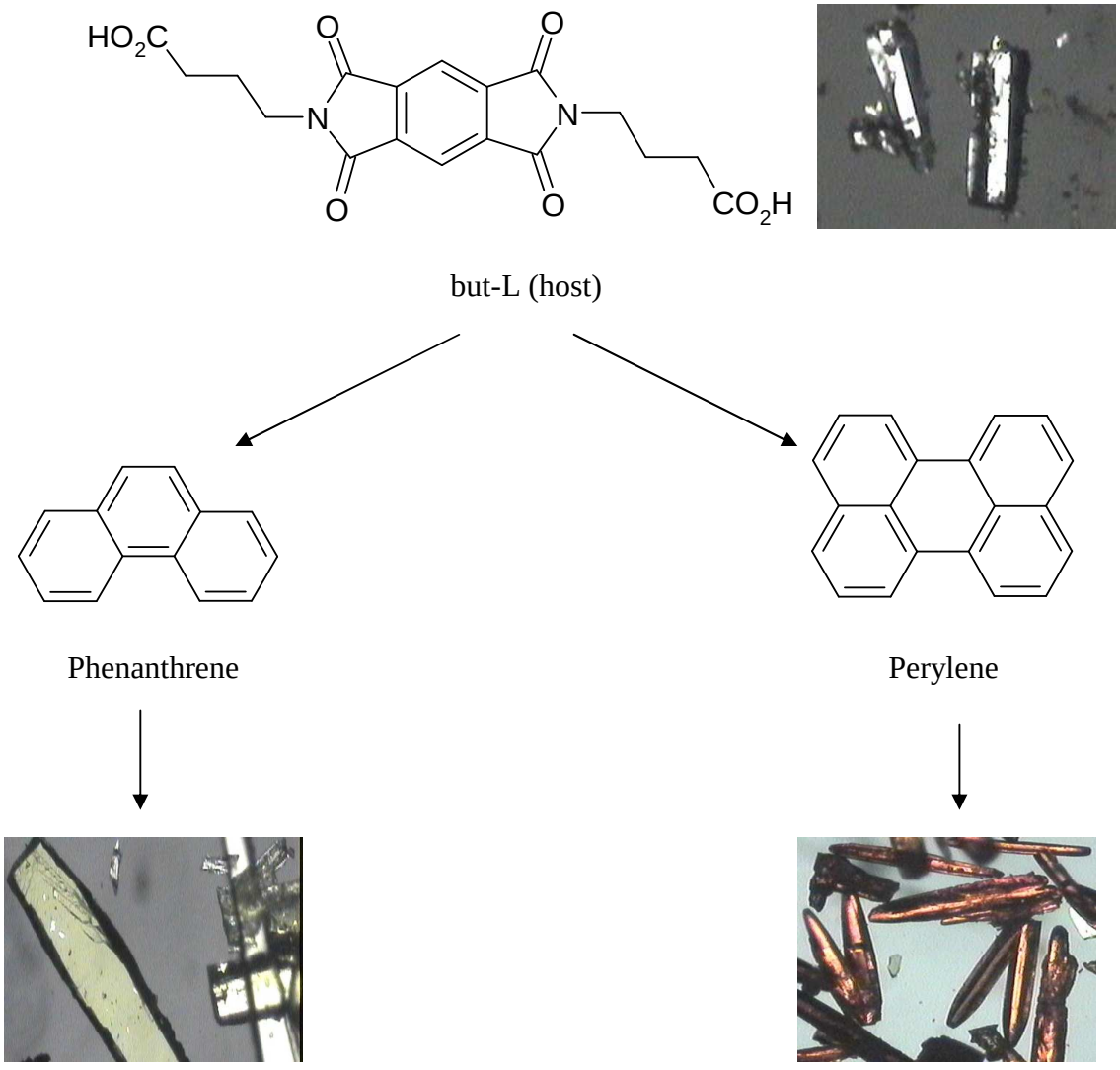

Figure 4.1: Optical microscope images at 50x magnification of but-L host molecule, with the addition of aromatics donors leading to CT complex formation.

CT complexes were formed in solution, as indicated by the colour change upon mixing of the starting materials, this colour was retained during crystal formation. Figure 4.1 shows that crystal morphology between the host and CT complexes were similar yielding needles of different sizes. Yields obtained for the CT complexes varied from 20 % for but-PHEN), to 60% for (but-PERY).

4.4 Single Crystal X-Ray Diffraction

In the pursuit of growing CT complexes with novel host molecules a new host molecule was synthesised and crystals successfully grown. This molecule but-L is structurally similar to gly-L, in that the molecule is very planar and contains an electrophilic aromatic ring. The only difference between these two ligands is the increase in chain length from two carbons to four in the butyric derivative. CT complexes containing phenanthrene and perylene aromatic systems were successfully grown and analysed via SCXRD. Crystallographic details are given in table 4.1 below.

Table 4.1: Crystallographic data for but-L and CT complexes.

Crystal	**But-L**	**but-PHEN**	**but-PERY**
Chemical formula	C_{18} H_{16} N_2 O_8	C_{32} H_{26} N_2 O_8	C_{38} H_{28} N_2 O_8
M_r (g.mol^{-1})	388.33	566.47	640.62
Temperature/K	173 (2)	173 (2)	173 (2)
Cell setting	Monoclinic	Triclinic	Orthorhombic
Space group	$P2_1/n$	P-1	*Pmna*
a/Å	4.9520 (7)	7.10340 (10)	10.3969 (5)
b/Å	19.231 (3)	10.4017 (2)	7.4468 (4)
c/Å	8.9345 (12)	10.6917 (2)	19.3130 (9)
α/°	90.00	117.6460 (10)	90.00
β/°	95.758 (7)	101.2110 (10)	90.00
γ/°	90.00	91.0470 (10)	90.00
V/Å^3	846.5 (2)	681.07 (2)	1495.28 (13)
Z, D_{calc}/g cm^{-3}	2, 1.523	2, 1.359	4, 1.423
μ/mm^{-1}, F(000)	0.122, 404	0.100, 287	0.101, 668
Crystal size/mm	0.574 × 0.216 × 0.19	0.47 × 0.29 × 0.29	0.36 × 0.12 × 0.06
Absorption correction	None	None	None
θ_{max}/°	28.27	28.00	27.99
h, k, l (min, max)	(-6, 6), (-25, 25), (-11, 11)	(-9, 9), (-13, 13), (-14, 14)	(-13, 13), (-9, 9), (-25, 21)
Reflections collected	11074	19637	11581
Unique reflections	2093	3292	1902
Observed reflections	1783	2736	1294
No. of parameters	128	255	126
R_{int}	0.0365	0.0474	0.0675
R_1 , wR_2	0.0379, 0.0937	0.0370, 0.1471	0.0536, 0.1020
R_1, wR_2 (all data)	0.0445, 0.0979	0.0566, 0.1545	0.0839, 0.1123
GoF	1.040	1.072	1.043
$\Delta\rho_{max}$, $\Delta\rho_{min}$ (e Å^{-3})	0.288, –0.206	0.572, -0.296	0.296, –0.226

The above table indicates that three structures crystallised in different crystal systems and space groups. Both complexes formed with but-L have centrosymmetric space groups, thereby suggesting commonality with regard to the packing arrangements within the unit cell. Amongst the two CT structures only but-PHEN contains the same space group and crystal system when compared to its equivalent gly-L structure. The unit cell parameters for the two structures are however very different. As in the previous chapter the host (but-L) molecule contains the highest crystal density.

4.5 Structural Analysis

4.5.1 *N,N'*-bis(γ-butyric)-pyromellitic diimide (but-L)

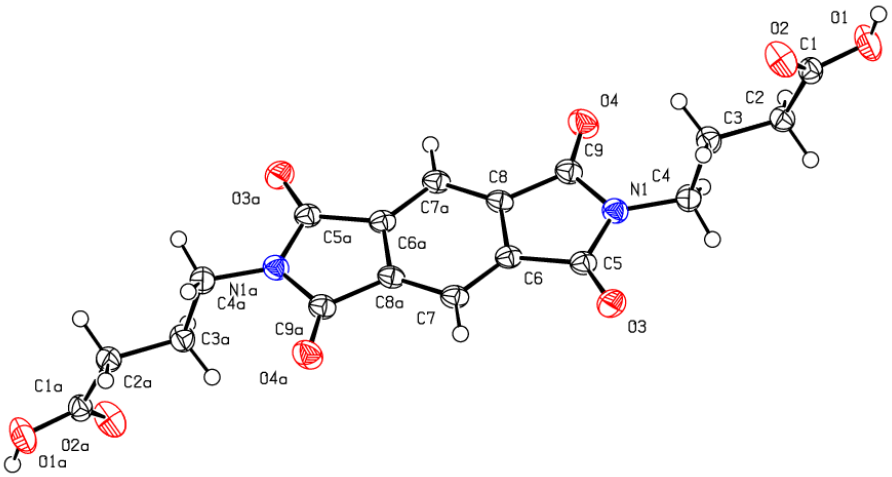

Figure 4.2: Ortep diagram of but-L drawn at 50% probability.

The but-L molecule crystallises as colourless blocky crystals in monoclinic $P2_1/n$. The molecules sits on an inversion centre and the unit cell contains 2 fold screw axes as well as a glide plane. It is structurally similar to gly-L with the addition of two extra carbons along each terminal carbon chain. It contains the same structural features as gly-L (*trans* arranged carboxylic acid groups, polar carbonyl groups and π acceptor sites), which makes it possible to undergo the formation of CT complexes.

The angle of the *trans* arrangement associated with the carboxylic acid groups increased from 112.08^{o} (gly-L) to 135.89^{o}

4.5.1.2 Hydrogen Bonding

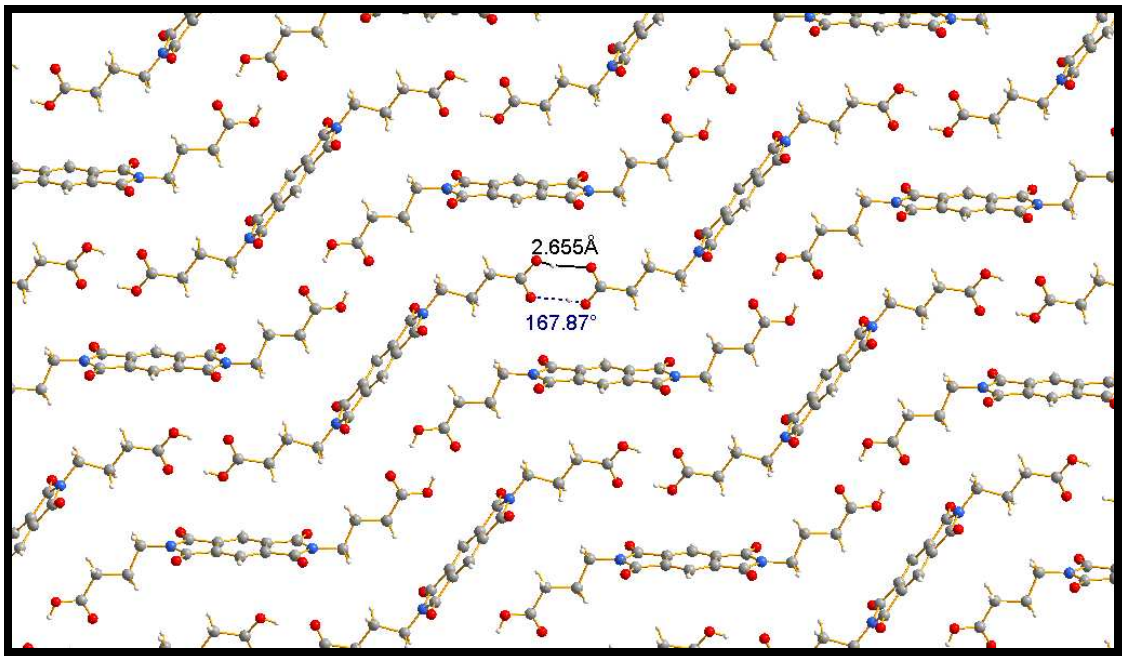

Figure 4.3: Two dimensional layers of but-L through hydrogen bonding of carboxylic acids, indicating zigzag arrangement within the 2D sheet.

but-L is an analogue of gly-L and as a result the carboxylic acid groups adopts a *trans* configuration. The *trans* configurations enables the structure to self assemble into one dimensional step-like ribbons through moderate inter-molecular hydrogen bonding through O1—H···O2 (d $_{O1\cdots O2}$ 2.655Å; ∟D—H···A 167.87°) leading to a $R^2_2(8)$ arrangement. Unlike gly-L, the extension of the 1D ribbons into the 2D sheets does not lead to offset stacking of the planar diimide rings. Instead it forms alternating 1D layers in which the carboxylate bridges sit above and below the diimide rings. This results in the formation of 2D zigzag arrangement of molecules within the crystal structure. It is however noted that the 3D extension of the structure indicates offset stacking of the diimide rings at an angle of 71.20° (C9H9---H9) and a inter planar distance of 3.17 Å. The overall (3D) extension of the structure occurs via

weak hydrogen bonding interactions between the planar diimide carbonyl groups and the alkyl chain. [C2—H_A···O4 (d $_{C2\cdots O4}$ 3.443Å; ∟D—H···A 135.25°), and C4—H_A···O3 (d $_{C4\cdots O3}$ 3.672Å; ∟D—H···A 129.45°)].

4.5.2 Charge Transfer Complexes

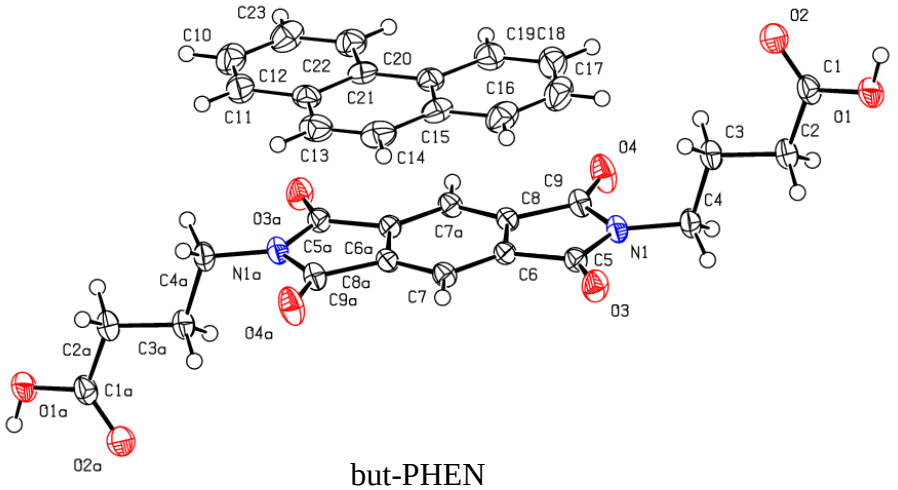

but-PHEN

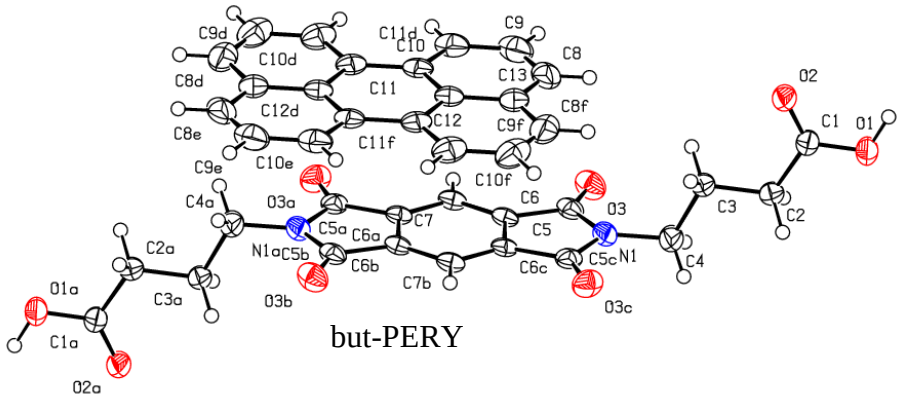

but-PERY

Figure 4.4: Ortep diagrams of grown CT complexes drawn at the 50% probability level.

As in the case of gly-L, CT complexes formed with but-L also yielded different colours with the different aromatic donor molecules - light yellow for but-PHEN and

orange for but-PERY. Both complexes form a 1:1 molecular complex with but-L, with neither structure containing any solvent molecules. Both CT complexes were centrosymmetric, with additional symmetry elements in the form of a glide plane, mirror plane, two fold screw axis and a two-fold rotation axis for but-PERY.

The angle of the *trans* carboxylic acids associated with the but-L host also deviated, due to CT formation. Angles differed by around two degrees between the host and the CT complexes with an angle of 133.96^{o} for but-PHEN and 137.13^{o} for but-PERY.

4.5.2.1 Hydrogen Bonding

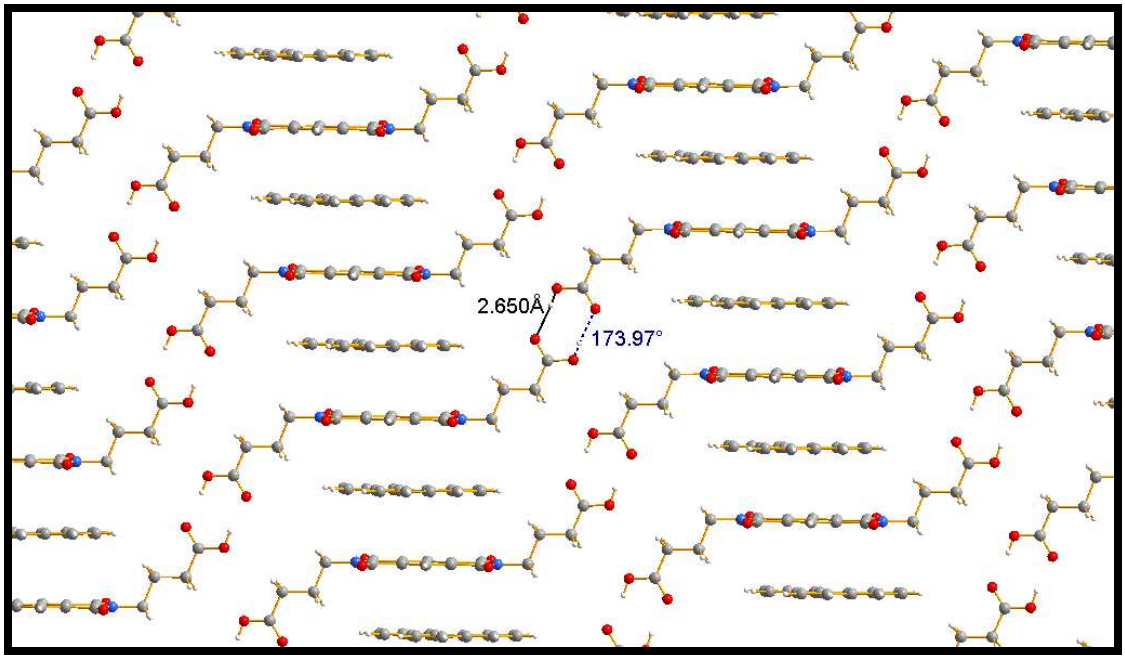

but-PHEN

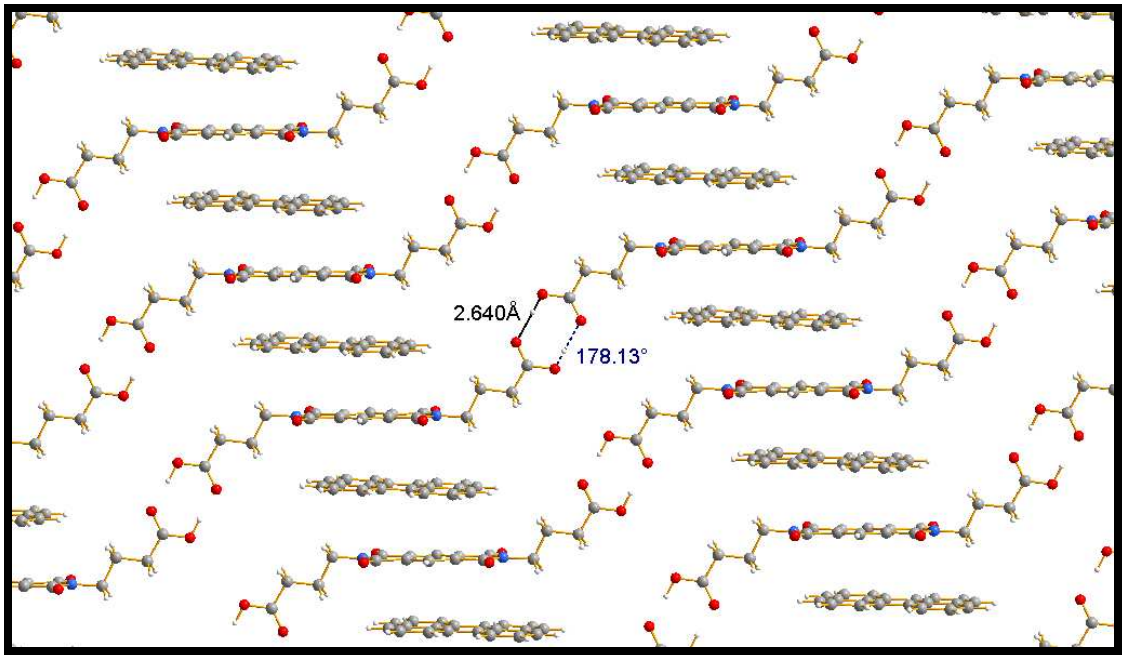

but-PERY

Figure 4.5: Two dimension layer formation through CT interactions and H-bonding.

CT complexes formed with but-L adopting the same 2D step-like stacking arrangement as gly-L CT complexes. This is due to charge transfer related interactions and moderate intermolecular hydrogen bonding between the terminal carboxylic acid groups, figure 4.5. Hydrogen bonding interactions present in both CT complexes led to the formation of a R^2_2 (8) hydrogen bonding ring pattern between the carboxylic acid groups. The phenanthrene molecules of the but-PHEN complex were found to be disordered over two positions resulting in alternate stacking arrangements of the phenanthrene molecule in this structure. Both CT complexes formed with but-L contain carboxylate bridges that were equidistant to each other, table 4.2. The 2D offset stacking arrangement indicates a decrease in the stacking angle between the two CT complexes from 75.13^o for but-PHEN to 65.77^o for but-PERY. This decrease was due to the increase in size of the aromatic donor.

Table 4.2: Intermolecular hydrogen bonding between but-L molecules in the CT complexes studied.

CT complex	Interaction	D—H/Å	H···A/Å	D···A/Å	∟D—H···A/°
but-PHEN	O1—H···O2	0.841	1.809	2.650(2)	173.97(7)
but-PERY	O1—H···O2	0.975	1.665	2.640(60)	178.13(30)

Both CT complexes are further stabilised by weak CH···O, CO···π and π···π interactions, between the host molecules (but-L–but-L) and the host guest molecules (but-L–aromatic). These interactions enable the structure to extend infinitely into the second and third dimension. Two dimensional extension is mainly stablised by CO···π interactions amongst the imide carbonyl and the aromatic donor molecules.

[C5—O3···*Cg*: $_{C\cdots\pi}$ 3.401Å; ∟D—H···A 73.58° and C5—O3···*Cg*: $_{C\cdots\pi}$ 3.474Å; ∟D—H···A 65.38° (but-PHEN) and C5—O3···*Cg*: $_{C\cdots\pi}$ 3.653Å; ∟D—H···A 78.76° (but-PERY)].

Table 4.3 Weak C-H···O interactions between but-L–but-L (b-b) and aromatic–but-L (a-b) groups in the two complexes reported here.

CT complex	Interaction	D—H/Å	H···A/Å	D···A/Å	∟D—H···A/°
but-PHEN (b-b)	C2—H···O4	0.990	2.516	3.506(2)	136.28(7)
but-PHEN (b-b)	C3—H···O3	0.990	2.572	3.562(2)	125.49(7)
but-PHEN (b-b)	C4—H···O4	0.990	2.623	3.613(2)	134.11(7)
but-PHEN(a-b)	C13—H···O2	0.950	2.682	3.632(3)	126.54(20)
but-PERY (b-b)	C2—H_A···O3	0.990	2.448	3.438(2)	113.93(10)
but-PERY (b-b)	C3—H_A···O3	0.990	2.656	3.646(2)	117.73(10)

Just as with gly-L CT complexes, the complexes formed with but-L also extend through step-like arrangements through moderate intermolecular hydrogen bonding. Thereby resulting in the formation of novel CT complexes. It was noted that but-PHEN is structurally related to gly-PHEN in the way it extends. Whilst but-PERY was structurally related to gly-ANT, in that the adjacent 2D layers were arranged in a zigzag orientation relative to each other due to CH···O interaction between the IC carbonyls and the alkyl chains of the ligand molecules.

All CT complexes contain π···π interactions which are responsible for the stacking arrangements found within each structure. Inter-planar π···π distances between the aromatic and the host molecules varied little amongst the CT complexes [but-PHEN (3.38Å and 3.44Å) and but-PERY (3.34Å)]. but-PHEN contains two different distances between the host and the aromatic donor due to the phenanthrene being disordered over two positions. All π···π interactions found within the CT complexes were within the typical range of 3.6Å as outlined by Hunter and co-workers (1990).

4.6 Lattice Energy Calculations

Lattice energy calculations were performed using the Oprop module of the OPiX program (Gavezzotti, 2003). From the energy calculations performed on the host (but-L) and CT complexes, values of -682.7kJ/mol were calculated for but-PERY, -612.10kJ/mol for but-PHEN, -487.20kJ/mol for but-L. An increase of about 50kJ/mol in lattice energies was found in all structures when compared to the equivalent gly-L structures. This energy increase is attributed to the increase in size of the but-L host molecule. The molecule-molecule interaction yielded from the Oprop calculation also indicated similar molecular arrangements found in gly-L and its complexes. These geometries adopted identical interactions found across the host and CT structures. Molecular arrangements coincided with CT π···π interactions (I), OH···O interaction between the carboxylic bridges (II), alkyl hydrogen's bonding to IC (III), and ArH bonding to the terminal carbonyls (IV). The sum of these main molecule-molecule interactions contribute the most to the lattice energy obtained in each calculation. The arrangement of these molecules with respect to the host molecule (black) is illustrated below using but-PERY as an example (figure 4.6) along with their respective energies (table 4.4).

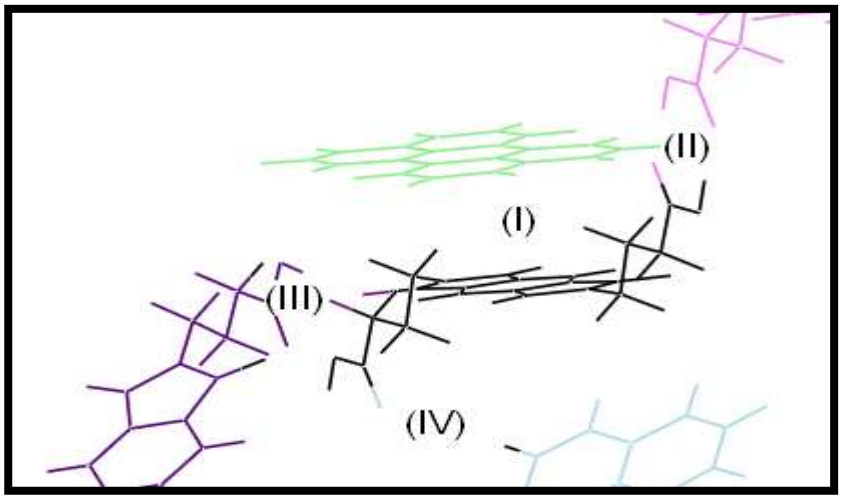

Figure 4.6: Structural arrangement of molecules for but-L CT complexes contributing most to the stability of the but-PERY structure.

Table 4.4: Energy values (kJ.mol^{-1}) associated with the most common molecular conformations adopted by all structures with but-L.

Structure		but-L	but-PHEN	but-PERY
Interaction				
(I)	π…π		-67.1 & -64.1	-82.3
(II)	CH···O	-41.5	-46.3	-47.0
(III)	CH···O	-25.9	-30.7 & -22.5	-22.9
(IV)	Ar-H···O		-14.0 & -10.8	-13.3

Table 4.4 indicates the various energies associated with the various molecule-molecule orientations adopted within the host and CT structures. Just as in the case of gly-PHEN, table 4.4 shows two energy values for interactions (I), (III) and (IV). This is due to the phenanthrene molecule being disordered over two positions due to the asymmetric shape of the molecule with each value representing one of these orientations. The but-L structure contributes an additional stabilising energy of -32.5 kJ/mol and -63.8kJ/mol and is due to the 2D and 3D offset stacking arrangements of the but-L molecules (figure A1.2).

The above table suggests a general trend with regard to stabilising interactions of molecular geometries. It was observed that the most stabilising interaction amongst all structures was due to an orientation of π···π interaction. The next most important contribution to the lattice energy was due to the arrangement of carboxylate bridges coinciding with OH···O interactions. This was followed by molecular arrangements associated with CH···O interactions experienced due to alkyl and IC carbonyl interactions, and ArH···O interactions between the aromatic ring and the terminal carbonyl groups. (See appendix for full list of molecule-molecule interactions).

4.7 Powder X-Ray Diffraction

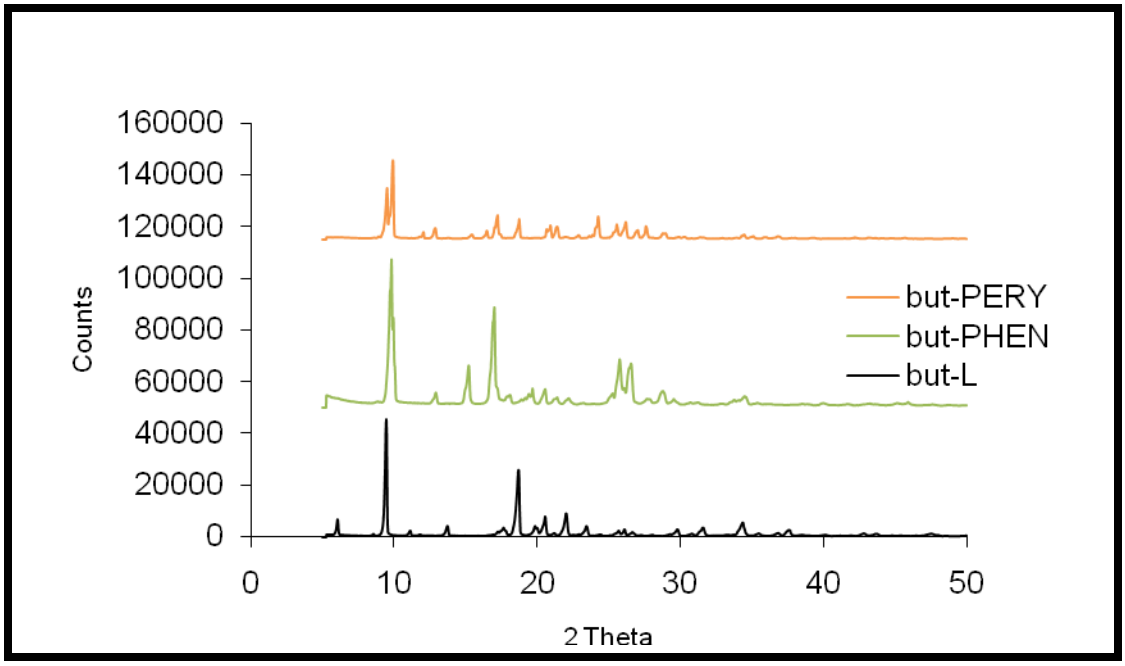

Figure 4.7: Experimental X-ray powder diffraction pattern of but-L and CT complexes.

The above PXRD data was obtained by grinding samples in air and running them in a Bruker D2 Phaser powder diffractometer. For all three samples, powder patterns calculated using the respective single crystal data were found to match the experimental powder patterns, as outlined in the appendix.

4. 8 Thermal Analysis

4.8.1 Thermogravimetric Analysis (TGA)

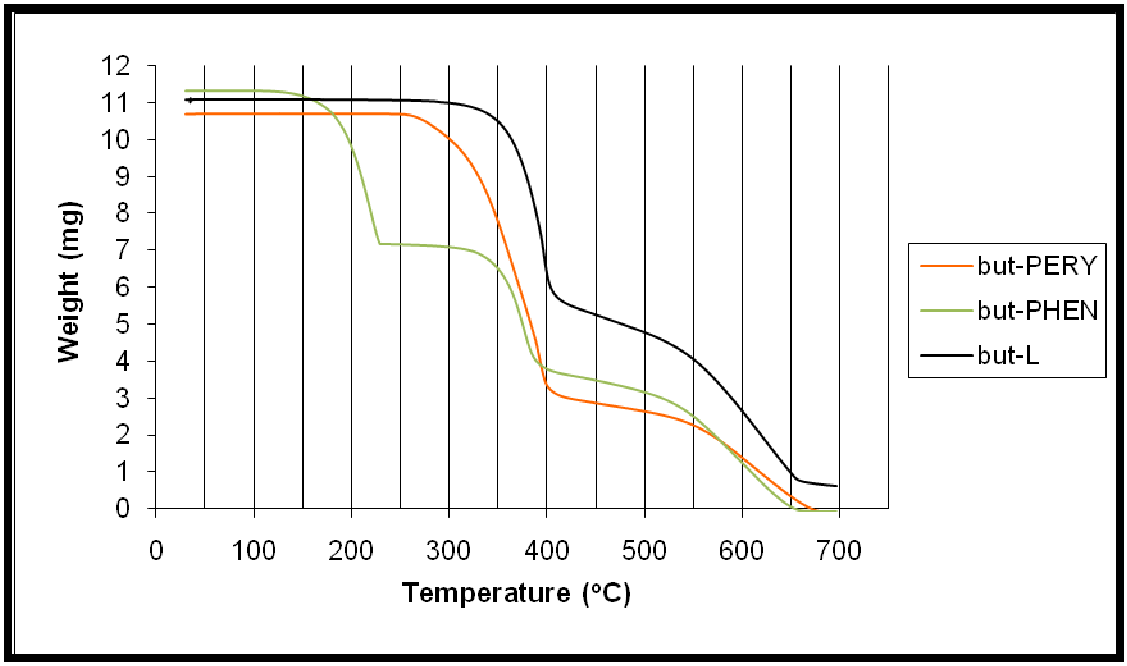

Figure 4.8: Thermogravimetric trace for but-L and CT complexes.

The TGA trace analysis shown in figure 4.7, illustrates variable degradation step arrangements for the but-L and CT complexes. The host material but-L showed a two step degradation pattern with a thermal stability to around 300^{o}C. This was accompanied by a weight loss of 51% (5.65mg) at higher temperatures, followed by an additional weight loss of 36% (3.99mg) at temperatures greater than 511^{o}C. The two CT complexes varied in thermal stability with but-PHEN being stable up to a temperature of 190^{o}C, followed by a weight loss of 36.8% (4.17mg), and 260^{o}C for but-PERY with a weight loss of 34% (3.63mg). As with the gly-CT complexes, the but-CT complexes also follow the degradation pattern of but-L between 300^{o}C and 650^{o}C, corresponding to a weight loss of 59.0% (6.68mg) and 63.0% (6.73mg) for but-PHEN and but-PERY respectively.

4.8.2 Differential Scanning Calorimetry (DSC)

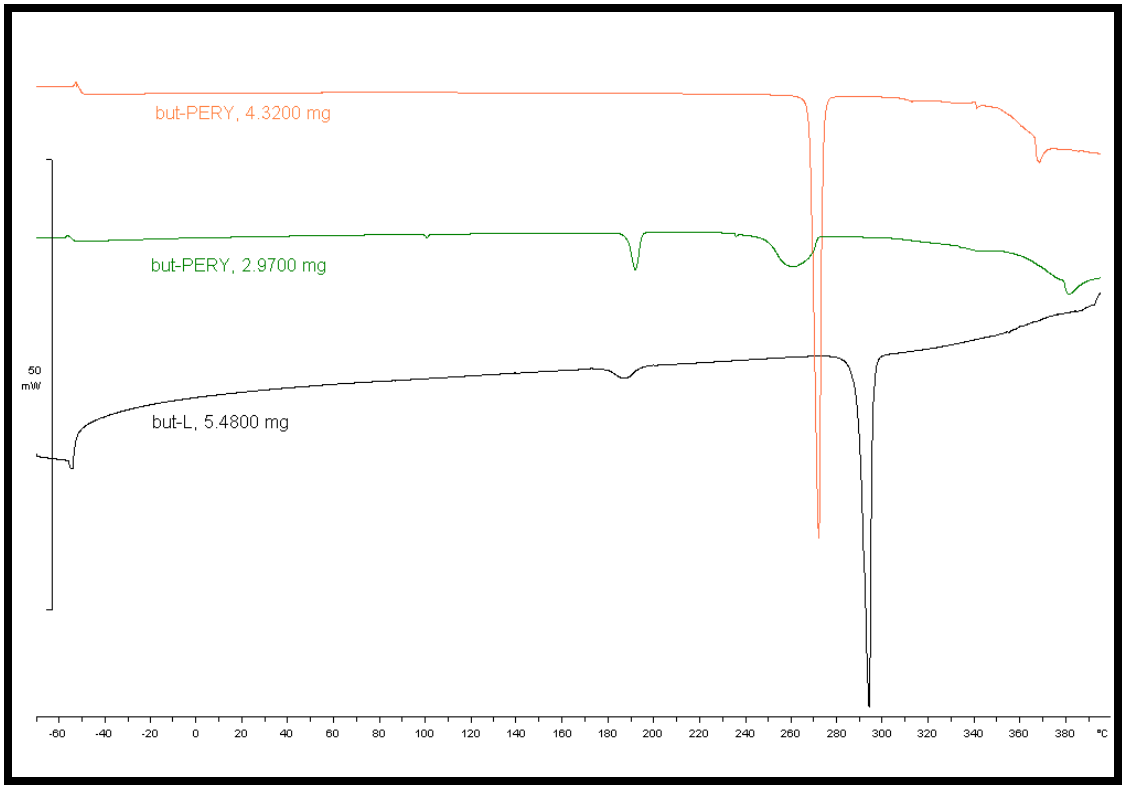

Figure 4.9: DSC traces of heat flow (mW) vs. temperature (^{o}C) for but-L and CT complexes.

The DSC scans above indicate two endotherm peaks for but-L, corresponding to a phase change at 184.26^{o}C (-3.94kJ/mol) and melting at 295.97^{o}C (-68.5kJ/mol) respectively. but-PHEN contains three endothermic peaks with the first peak occurring at 94.67^{o}C corresponding to an energy of -0.75kJ (phase change), followed by the degradation of the CT complex due to the liberation of the aromatic donor at 183.33^{o}C (-19.6kJ/mol) and the removal of but-L at 245.02^{o}C (-59.5kJ/mol). Once again the CT complex formed with perylene only shows one peak at 265.94^{o}C and corresponded to -152kJ/mol energy due to the melting of the CT complex. The melting points obtained from the DSC were in good correlation with the TGA data.

4.9 Spectral Analysis

4.9.1 Solid state UV-Vis

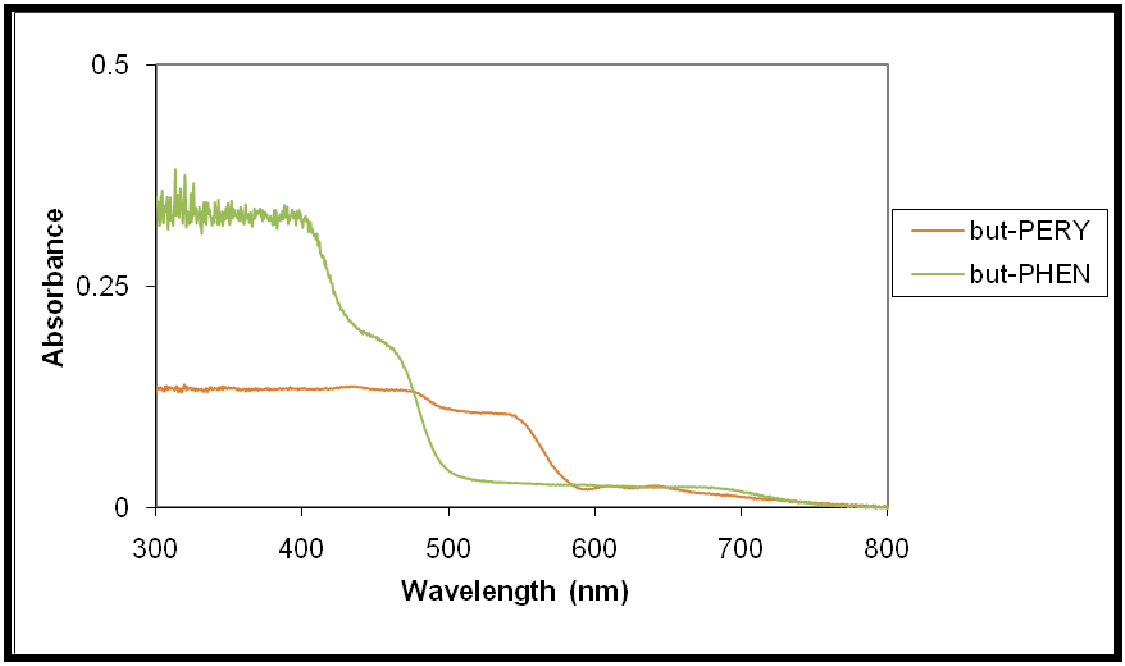

Figure 4.10: Solid state UV-Vis absorption spectra for but-L CT complexes.

Figure 4.10 indicates the formation of CT bands using but-L as a host molecule. Both CT complexes form 2 CT transition bands with the larger aromatic donor (perylene) occurring at the higher wavelengths (592nm and 499nm). The wavelengths associated with but-PERY corresponded to energies of 240kJ/mol and 202kJ/mol respectively.

4.9.2 Liquid state UV-Vis

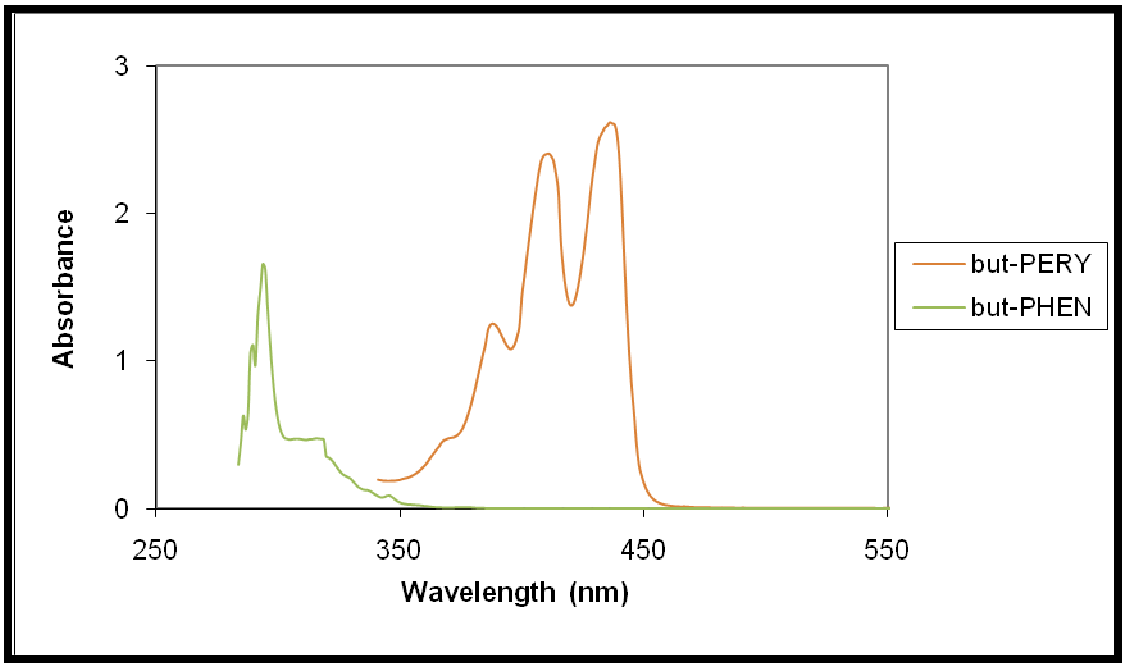

Figure 4.11: UV-Vis absorption spectra for but-L CT complexes carried out in solution.

Figure 4.11 shows the UV-Vis spectra of CT complexes formed with but-L in solution. The spectra obtained was consistent with the data obtained for the CT complexes formed with gly-L, in that the but-PHEN contains two absorbance bands between 280-340nm while but-PERY contains three bands at 350-450nm.

As seen in the previous chapter, the liquid and solid spectra indicate different absorption energies of the CT complexes, with the solid state spectra indicating much lower absorption energies than the liquid states.

4.9.3 IR-Spectrum

Table 4.5: Infrared spectral data of but-L and CT complexes.

Complexes	Ar (C−H) (donor)	Ar (C−H) (acceptor)	C=O	C-N	COOH	$C-H_2$
but-L	725S	806S	1699S	1033S	1699S & 1286M	1357 & 1392M
but-PHEN (cm^{-1})	727S	804 -806M	1691S	1035M	1691S &1286M	1367-1392M & 1430W
but-PERY (cm^{-1})	725 & 767S	806S	1699S	1033 S	1699S &1286M	1357-1394M

The above table indicates the ranges of spectral bands assigned to but-L and CT complexes. Each assignment was within the expected ranges as given in table 3.7. Each spectrum appears to be very similar relative to each other, and the assignments are consistent with the general structure of the host and the but-CT complexes. Once again the perylene complex indicates the presence of an additional C-H aromatic donor.

4.10 Further Experimentation

The successful synthesis and characterisation of a new host molecule allowed for the formation of new CT complexes. However beside the two complexes formed no others could be obtained. The use of naphthalene and anthracene as aromatic donors did not yield any results. Methods included using 2:1 donor: acceptor ratios in the appropriate solvents, as well as using various solvents to dissolve the aromatic donor and layering onto a DMF solution containing the host molecule. These methods did not work. However it is believed that larger ring donors (>5 rings) would readily have led to the formation of CT complexes; however these molecules are be difficult to use due to solubility issues.

4.11 Discussion

In pursuit of the forming new acceptor molecules, but-L molecules was successfully synthesised and utilised in the formation of CT complexes. Two new CT complexes

were successfully grown using phenanthrene and perylene as donor molecules. Both complexes contained the same crystal morphology with colours varying from yellow (phenanthrene) to orange (perylene). Again this difference in colour was due to difference in electronic charge being transferred from a donor to an acceptor molecule, and is dependant of the size, shape and conjugation of the donor molecule. SCXRD and various other analytical techniques were carried out to better understand the physical and chemical properties of these materials.

SCXRD indicated that all three structures crystallised out in different crystal systems. The host but-L structure crystallised out in a monoclinic $P2_1/n$ system, with the two CT complexes crystallising in a triclinic *P*-1 system (but-PHEN) and an orthorhombic *Pmna* system (but-PERY). The CT complex structures showed a 1:1 donor acceptor ratio, with all structures containing a hydrogen bonded graph set of $R^2_2(8)$. This hydrogen bonding pattern amongst the carboxylate groups of the host molecule enabled each structure to extend in a step like arrangement. Amongst the CT complexes only gly-PHEN contained intermolecular hydrogen bonding between the donor and acceptor molecules, as well as displaying asymetric π stacking due to the shape of the donor molecule leading to it being disordered over two positions. This also yields different interplanar π···π distances of 3.38Å and 3.44Å respectively. The inter-planar π···π distance associate with but-PERY was 3.34Å and all π···π distance were within the limit outlined by Hunter (1990).

It was observed that the overall structure extension of the CT complexes differed when compared the host molecule. The host but-L arrangement was made up of zigzag arrangement of host molecules within the 2D sheets (figure 4.3). This formation was due the carboxylate bridges sitting above/below the diimide rings, thereby resulting in 2D zigzag arrangement of molecules. Both CT complexes adopted a parallel arrangement of molecules within the 2D sheets. The overall 3D extension of all structures occurs through various weak hydrogen bonding interactions amongst the host-host and host-guest (aromatic ring, carbonyls groups

and alkyl chains). Each CT structure also adopted different 3D arrangements, but-PHEN adopting an arrangement found within gly-PHEN, with the parallel arrangement of adjacent 2D sheets, whilst but-PERY adopted an 3D arrangement found in gly-ANT, forming zigzag 2D sheets.

Lattice energy calculations revealed that the most stable structure was but-PERY with an energy of -682.7kJ/mol, followed by but-PHEN (-612.10 kJ/mol), and lastly but-L (-487.20 kJ/mol). There were four common molecular arrangements corresponding to stabilising interactions found amongst the CT complexes. These included π···π stacking, and various hydrogen bond interactions.

The PXRD data indicated that the simulated and observed patterns were very similar. Peak intensity differed due to preferred orientation adopted by the molecules.

Both the TGA and DSC data correspond well when compared to each other. Each method indicated an increase in thermal stability and melting, as the size of the donor molecule increased. Both the host and but-PHEN indicated a phase transition at their respective temperatures.

Solid state UV-Vis indicated that the larger aromatic donor contained the lowest transition energies. Both the solid UV-Vis and liquid state UV-Vis differed when compared to each other indicating the effect of the crystal environment versus the liquid environment on such spectra. The IR spectrum for but-L and CT complexes showed that all peaks are within the expected ranges and are consistent with the general structure of host molecule and CT complexes.

4.12 References

Barooah, N., Sarma, R. J., Batsanov, A. S., Baruah, J. B. (2006). J. Molecular Structure, 8, 608.

Hunter, C. A., Sanders, J. K. M. (1990) J. Am. Chem. Soc. 112, 5525

Park, L. Y., Hamilton, D.G., McGehee, E. A., McMenimen K. A. (2003). J. Am. Chem. Soc., 125, 10586.